Note: This copy is for your personal non-commercial use only. To order presentation-ready copies for distribution to your colleagues or clients, contact us at www.rsna.org/rsnarights.

Early Small-Bowel Ischemia: Dual-Energy CT Improves Conspicuity Compared with Conventional CT in a Swine Model[1]

Theodora A. Potretzke, MD
Christopher L. Brace, PhD
Meghan G. Lubner, MD
Lisa A. Sampson, BS
Bridgett J. Willey, MS
Fred T. Lee, Jr, MD

Purpose: To compare dual-energy computed tomography (CT) with conventional CT for the detection of small-bowel ischemia in an experimental animal model.

Materials and Methods: The study was approved by the animal care and use committee and was performed in accordance with the Guide for Care and Use of Laboratory Animals issued by the National Research Council. Ischemic bowel segments (n = 8) were created in swine (n = 4) by means of surgical occlusion of distal mesenteric arteries and veins. Contrast material–enhanced dual-energy CT and conventional single-energy CT (120 kVp) sequences were performed during the portal venous phase with a single-source fast-switching dual-energy CT scanner. Attenuation values and contrast-to-noise ratios of ischemic and perfused segments on iodine material–density, monospectral dual-energy CT (51 keV, 65 keV, and 70 keV), and conventional 120-kVp CT images were compared. Linear mixed-effects models were used for comparisons.

Results: The attenuation difference between ischemic and perfused segments was significantly greater on dual-energy 51-keV CT images than on conventional 120-kVp CT images (mean difference, 91.7 HU vs 47.6 HU; $P < .0001$). Conspicuity of ischemic segments was significantly greater on dual-energy iodine material–density and 51-keV CT images than on 120-kVp CT images (mean contrast-to-noise ratios, 4.9, 4.3, and 2.1, respectively; $P < .0001$). Although attenuation differences on dual-energy 65- and 70-keV CT images were not significantly different from those on 120-kVp images (55.0 HU, 45.8 HU, and 47.6 HU, respectively; 65 keV vs 120 kVp, $P = .15$; 70 keV vs 120 kVp, $P = .46$), the contrast-to-noise ratio was greater for the 65- and 70-keV images than for the 120-kVp images (4.4, 4.1, and 2.1 respectively; $P < .0005$).

Conclusion: Dual-energy CT significantly improved the conspicuity of the ischemic bowel compared with conventional CT by increasing attenuation differences between ischemic and perfused segments on low–kiloelectron volt and iodine material density images.

©RSNA, 2014

[1] From the Departments of Radiology (T.A.P., C.L.B., M.G.L., L.A.S., B.J.W., F.T.L.), Biomedical Engineering (C.L.B.), and Medical Physics (C.L.B.), University of Wisconsin-Madison, E3/366 Clinical Science Center, 600 Highland Ave, Madison, WI 53792. Received April 13, 2014; revision requested May 21; revision received July 14; accepted August 12; final version accepted September 17. **Address correspondence to** T.A.P. (e-mail: *theodora.nemeth@gmail.com*).

©RSNA, 2014

Acute bowel ischemia is a life-threatening abdominal emergency with reported mortality rates of 59%–93% (1). The clinical presentation is often nonspecific, with considerable symptom overlap with other acute abdominal conditions. Prompt surgical intervention remains the primary treatment choice but is less effective in patients with prolonged symptoms or a delay in diagnosis. In a study of 72 patients who underwent surgical intervention for acute mesenteric ischemia, Kougias et al (2) reported 14% mortality if surgery was performed less than 12 hours after symptom onset and 72% mortality if surgery was performed more than 12 hours after symptom onset.

Computed tomography (CT) is the most useful first-line diagnostic test to evaluate patients suspected of having bowel ischemia. Although multidetector contrast material–enhanced CT (with CT angiography) has shown high sensitivity in the diagnosis of acute bowel ischemia, several of the most common signs are nonspecific, including bowel wall thickening, bowel dilatation, mesenteric stranding, and mesenteric fluid. However, bowel wall hypoenhancement, the CT sign with the highest specificity (93%–100%), may go unrecognized (3–8). Recognition of bowel wall hypoenhancement may be especially valuable early in acute presentation, when late secondary signs of infarction (both clinical and radiographic) have not yet developed. It is at this time that intervention may have the greatest potential for salvage of the bowel and preservation of life.

Advance in Knowledge

- The attenuation difference between ischemic and perfused bowel segments was significantly greater on dual-energy 51-keV CT images than on conventional 120-kVp CT images ($P < .0001$); the ischemic bowel showed higher contrast-to-noise ratios at dual-energy CT than at conventional CT (contrast-to-noise ratio, 4.9 vs 2.1, respectively; $P < .0001$).

Dual-energy CT is particularly useful for situations in which subtle differences in contrast enhancement may have important clinical implications. The attenuation of iodine is dependent on energy and increases at lower energy levels (approaching the K-edge of iodine) because of the predominance of the photoelectric effect (9,10). Therefore, iodine-containing tissue (ie, perfused) is hyperattenuating compared with noniodine-containing (ie, nonperfused) tissue at lower energy levels but not at higher energy levels (11,12). There is greater attenuation difference between perfused and nonperfused tissue at lower energy levels, resulting in improved conspicuity of hypoenhancing tissue.

Another important advantage of dual-energy CT compared with conventional CT is the ability to create a map of material pairs, such as iodine and water, because of the markedly different absorption spectra of soft tissue and iodine. In addition, virtual monospectral images at a single kiloelectron volt level near the K-edge of iodine can be created from a dual-energy CT data set to increase sensitivity to iodine. Despite the increasing use and accessibility of dual-energy CT technology, investigation of dual-energy CT for the diagnosis of bowel ischemia has been limited. The purpose of our study was to compare dual-energy CT to conventional CT for the detection of small-bowel ischemia in an experimental animal model.

Materials and Methods

Animal Preparation

The study protocol was approved by the animal care and use committee of our institution and the study was performed in accordance with the Guide for Care and Use of Laboratory Animals issued by the National Research Council (13). Four female domestic swine (mean weight, 68 kg) were used for this study (University of Wisconsin Agricultural Research Station, Arlington, Wis). Before administration of anesthetic, sedation was achieved with 7 mg/kg of intramuscularly administered tiletamine hydrochloride and zolazepam hydrochloride (Telazol; Wyeth, Fort Dodge, Iowa) and 2.2 mg/kg of xylazine hydrochloride (Xyla-Ject; Phoenix Pharmaceutical, St Joseph, Mo). Endotracheal intubation was performed in the standard fashion, facilitated by administration of 0.05 mg/kg of atropine (Phoenix Pharmaceutical). Anesthesia was then induced and maintained with 2% inhaled isoflurane (Halocarbon Laboratories, River Edge, NJ) to effect. Animals were placed in a supine position on the bed of a CT scanner. Once the animals were anesthetized, laparotomy was performed via a vertical midline incision.

Induction of Bowel Ischemia

The study was performed between January 31, 2013 and May 23, 2013. Surgical induction of bowel ischemia was performed with the animal on the CT scanner bed. Eight total segments of ischemia were induced, two in each animal. With the abdomen open, an approximately 10-cm segment of small bowel was selected and exteriorized. Then, the distal mesenteric arteries

Implication for Patient Care

- Dual-energy CT may improve early detection of bowel ischemia by increasing the conspicuity of hypoenhancing bowel segments on low–kiloelectron volt and iodine material density images.

Published online before print
10.1148/radiol.14140875 **Content codes:** CT GI

Radiology 2015; 275:119–126

Abbreviations:
CNR = contrast-to-noise ratio
ROI = region of interest

Author contributions:
Guarantors of integrity of entire study, T.A.P., C.L.B., L.A.S., F.T.L.; study concepts/study design or data acquisition or data analysis/interpretation, all authors; manuscript drafting or manuscript revision for important intellectual content, all authors; approval of final version of submitted manuscript, all authors; agrees to ensure any questions related to the work are appropriately resolved, all authors; literature research, T.A.P., M.G.L., F.T.L.; clinical studies, T.A.P., B.J.W.; experimental studies, all authors; statistical analysis, T.A.P., C.L.B.; and manuscript editing, all authors

Conflicts of interest are listed at the end of this article.

and veins supplying and draining this segment were ligated en bloc with a single surgical suture through the mesentery (Fig 1). This resulted in complete occlusion of the arterial inflow and the venous drainage of this segment. Then, the bowel was returned to the abdomen. The two segments in each animal were chosen from separate quadrants of the abdominal cavity.

The efficacy of our technique of ischemia induction was confirmed in our early animals by means of pre- and postligation ultrasonography (US) (Fig 2). We obtained color- and pulsed-wave spectral Doppler US images with the transducer (and a small amount of coupling gel) placed directly on the bowel segment in transverse and longitudinal planes. A US unit (Acuson S2000; Siemens Medical, Malvern, Pa) with an L18 probe at 15 MHz was used with settings selected for superficial soft-tissue imaging (breast imaging presets). Sonographically detectable blood flow was documented in the bowel wall before the induction of ischemia. Immediately after the mesenteric ligation, the absence of blood flow was documented in the same bowel segments. Visual inspection after induction of ischemia also was considered to be confirmatory of ischemia, because the bowel tissue developed visible duskiness at approximately 1–2 minutes after ligation.

CT Data Acquisition

Each swine underwent contrast-enhanced CT less than 15 minutes after the induction of bowel ischemia. CT scanning was performed with a single-source unit that could scan in dual-energy mode with rapid switching between 80 and 140 kVp or in a conventional mode, with a single 120-kVp beam image (Discovery 750 HD; GE, Waukesha, Wis). The scanning mode was quickly switched between dual-energy mode and conventional mode. Simulated monoenergetic and iodine material density images were created from the 80- and 140-kVp data sets by means of basis pair material decomposition by using the scanner's quantitative dual-energy CT data processing technology (Gemstone Spectral Imaging, GE). Simulated

Figure 1

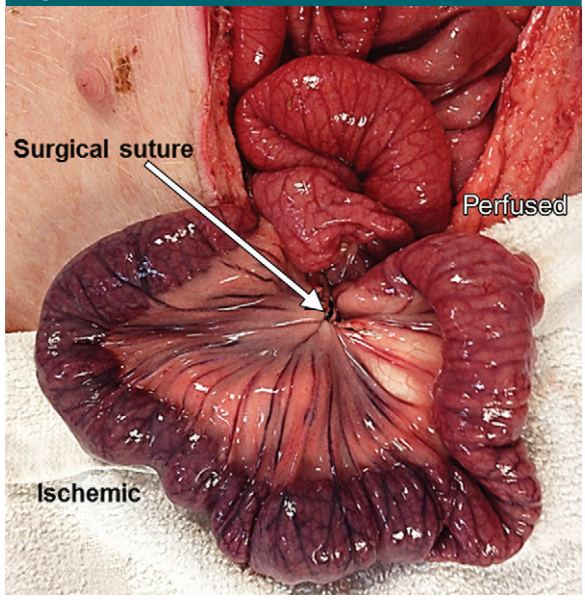

Figure 1: Photograph of segment of swine small bowel after placement of suture through mesentery to ligate distal mesenteric arteries and veins supplying and draining this bowel segment. Duskiness of ischemic segment relative to perfused segment indicates early ischemia.

Figure 2

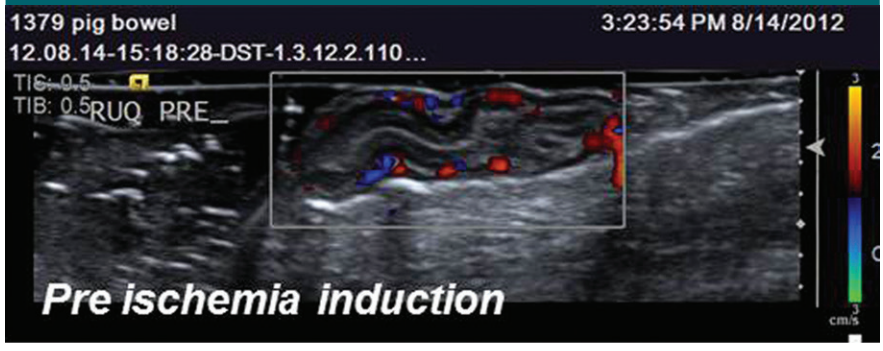

a.

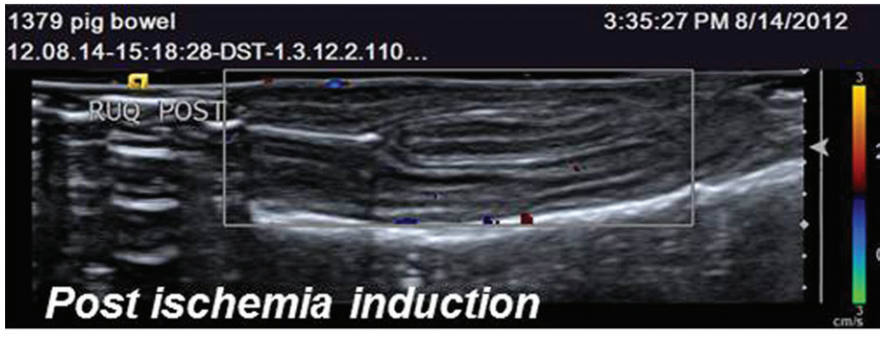

b.

Figure 2: Color Doppler US images before and after induction of ischemia. Normal color flow is seen in bowel wall on **(a)** preinduction image but is absent on **(b)** postinduction image.

monoenergetic images were available in 1-keV increments between 40 and 140 keV on the scanner workstation.

Each animal was imaged with both dual-energy and conventional 120-kVp CT in a crossover design. Animals 1 and 3 underwent conventional 120-kVp scanning in the portal venous phase and immediate dual-energy scanning in the late portal venous phase. Animals 2 and 4 underwent dual-energy portal venous phase scanning and then immediate late portal venous phase conventional 120-kVp scanning. Portal venous and late portal venous scanning was performed at approximately 70 and 100 seconds after contrast material administration, respectively. This design allowed direct comparison of conventional and dual-energy scanning without bias in the imaging timing.

We limited our data collection to the portal venous phase on the basis of the results of an earlier pilot study (14) that included the arterial, portal, and delayed phases. In that study, conspicuity of the ischemic bowel segments was high in the portal venous and delayed phases compared with that in the arterial phase. The portal venous phase is the most common phase of acquisition for clinical abdominal CT.

In each animal, a total volume of 125 mL of iohexol at a concentration of 300 mg of iodine per milliliter (Omnipaque 300, GE Medical) was injected at a rate of 5 mL/sec. After scanning was complete, animals were sacrificed by using an intravenous injection of 0.2 mL/kg of 390 mg/mL of pentobarbital sodium and 50 mg/mL of phenytoin sodium (Beuthanasia-D; Schering-Plough, Kenilworth, NJ).

Image Analysis

Images were reviewed by using an image viewer (Gemstone Spectral Image Viewer; GE Medical). Images acquired in dual-energy mode were reconstructed on the workstation at monochromatic viewing energy levels of 51, 65, and 70 keV. The 65- and 70-keV energy levels were chosen because they approximate the spectral center of a 100–120-kVp polychromatic beam. Iodine material density images also were created from the dual-energy data for each animal. Images acquired in conventional mode were reviewed on the same workstation.

Statistical Methods

Small regions of interest (ROIs) were manually placed on the bowel wall of the ischemic and adjacent perfused segments by a single observer (T.A.P., with 4 years of experience) who established a method in consensus with a second observer in the pilot study (M.G.L., with 10 years of experience) (Fig 3). One measurement was made per segment. The ROIs were variable in their shape and size due to the variability in the thickness of the bowel wall and the degree of luminal distention. Both circular and oval ROIs were used. A typical circular ROI had a diameter of approximately 8 mm and an area of 50 mm^2. Attenuation values (in Hounsfield units) and iodine material density (in milligrams of iodine per cubic centimeter) were recorded in the ROIs. Standard deviations of attenuation values in the ROI were recorded to represent image noise. Contrast-to-noise ratios (CNRs) were calculated for each ischemic segment to quantify the visibility of the ischemic segment relative to the perfused segment by using the following equation: CNR = (AVPB − AVIB)/[(SDPB + SDIB)/2], where AV is the attenuation value, PB is the perfused bowel, IB is the ischemic bowel, and SD is the standard deviation of the attenuation value. The attenuation of the bowel wall, iodine concentration as calculated by using the quantitative dual-energy CT technology of the scanner, and CNR were compared among energy levels.

Summary descriptive statistical measures were obtained for attenuation and CNR for ischemic and perfused segments for each energy level. Linear mixed-effects models (15,16) were used to model attenuation change as a function of image energy as a fixed effect, with a pig-dependent random intercept term. The different energy levels were considered as categorical (instead of quantitative) variables. A P value of less than .05 (two sided) was considered to indicate a significant difference. Exploratory and diagnostic plots were obtained to assess possible violations in model assumptions. All statistical graphics and models were generated by using software (R 3.0.1; [17]).

Figure 3

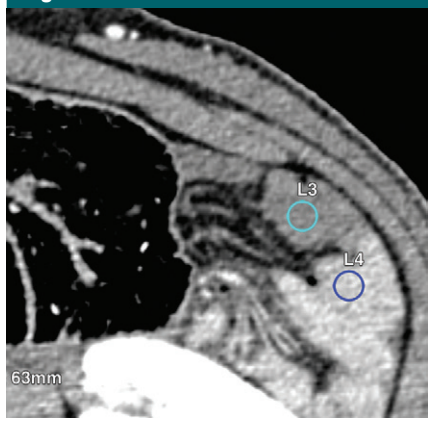

Figure 3: Contrast-enhanced 51-keV monospectral CT image shows sample circular ROIs on bowel wall of adjacent ischemic *(L3)* and perfused *(L4)* segments.

Results

There was no significant difference in bowel wall attenuation or CNR between portal venous and immediate late portal venous phases after administration of contrast material (P = .47 and P = .77, respectively). Therefore, these data were analyzed together and both were considered to be the portal venous phase. In general, the attenuation difference between images of ischemic and perfused segments was inversely correlated with the dual-energy CT energy reformatting (in kiloelectron volts). The attenuation difference between ischemic and perfused segments was greatest at 51 keV and was significantly higher than that on the conventional 120-kVp images ($P < .0001$). The attenuation difference between ischemic and perfused segments at 65 and 70 keV was lower than that at 51 keV and was not significantly different from that on conventional CT images (P = .15 and P = .46 respectively).

Conspicuity of ischemic segments was significantly greater on dual-energy iodine material density and 51-keV images than that on conventional CT images (mean CNR in the portal venous phase, 4.9, 4.3, and 2.1, respectively; $P < .0001$) (Figs 4, 5). Despite the similarity of the bowel wall attenuation between conventional 120-kVp and 65- and 70-keV monospectral reconstructions from the dual-energy data, the CNR was greater for the 65- and 70-keV images than for conventional 120-kVp images (4.4, 4.1, and 2.1, respectively; $P < .0005$) due to the decreased noise on the monospectral 65- and 70-keV images compared with that on the conventional images. Additional attenuation data are summarized in the Table.

Discussion

The diagnosis of small-bowel ischemia remains challenging, especially early in its course when late findings of bowel infarction such as pneumatosis and portal venous gas have not yet appeared. The correct diagnosis of early bowel ischemia and subsequent appropriate surgical referral are often dependent on the radiologist's ability to recognize subtle findings on conventional CT images.

In this study, we showed that dual-energy CT significantly increased bowel wall attenuation differences between perfused and ischemic segments compared with those of conventional CT, and thereby improved the conspicuity of segmental bowel wall hypoenhancement. The attenuation difference between perfused and ischemic segments on 51-keV images was nearly double that on the conventional 120-kVp images. The attenuation difference on conventional CT images was nearly equivalent to that at 65 and 70 keV based on mean attenuation values and the lack of statistically significant differences among these groups. This was not surprising, because the spectral center of a conventional 120-kVp polychromatic beam is at approximately 65–70 keV. CNR also improved significantly with the use of dual-energy CT owing to this improved contrast and to decreased noise. The quantification of iodine in the bowel wall (iodine material density), a technique only available when scanning with dual-energy CT, also allowed for significant improvement in the conspicuity of ischemic segments compared with that with conventional scanning.

The improved conspicuity of segmental bowel wall hypoenhancement at dual-energy CT reduced the subtlety of what recently was shown to be the most accurate sign of intestinal ischemia. In a study (8) of 44 patients treated surgically for small-bowel obstruction, segmental bowel wall hypoenhancement showed sensitivity of 78% and specificity of 96% for ischemia when images were reviewed retrospectively. Seven cases of surgically proven bowel ischemia were missed at prospective interpretation, and in three of these cases, segmental bowel wall hypoenhancement went unrecognized. The increased conspicuity of bowel wall hypoenhancement with dual-energy CT could result in improved visibility of the ischemic bowel and higher radiologist confidence.

Previous authors (18–21) have suggested potential applications of dual-energy CT for the evaluation of bowel abnormalities, most commonly for the detection of hyperemia in patients with inflammatory bowel disease. De Cecco et al (22), in their review of oncologic applications of dual-energy CT, included one case of bowel ischemia imaged with dual-energy CT that showed improved visibility of bowel wall hypoenhancement on the iodine map. Our results

Figure 4

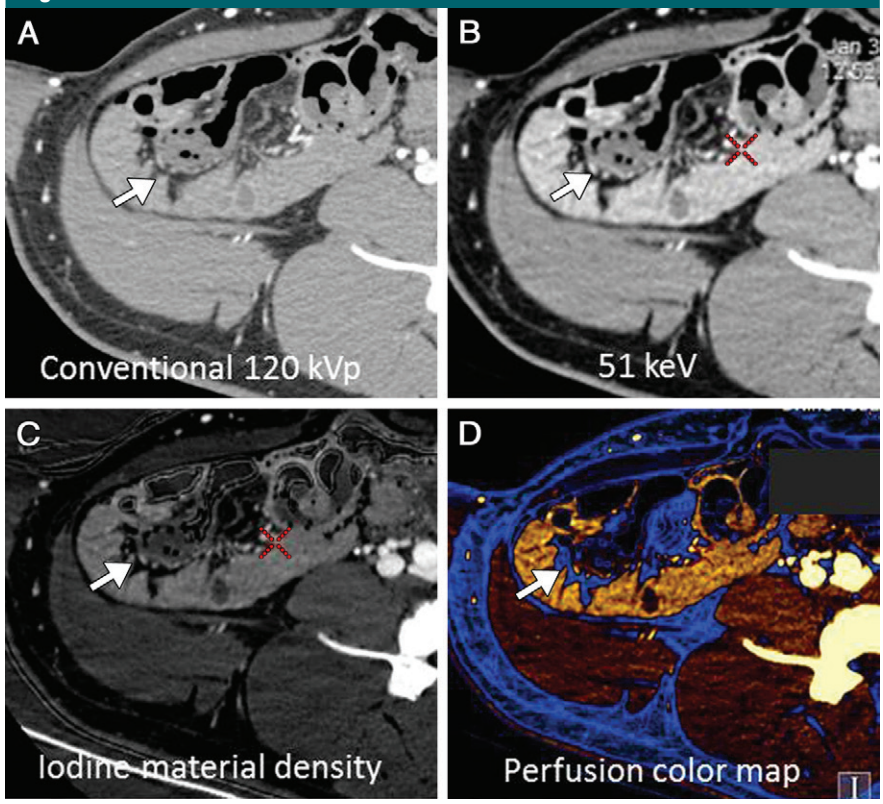

Figure 4: Axial and coronal contrast-enhanced CT images in early and late portal venous phases show ischemic segment of swine small bowel in right lower quadrant (arrows) that is less conspicuous on, *A*, single-energy conventional 120-kVp image, than on, *B*, dual-energy image reconstructed at virtual monoenergetic 51-keV, and, *C*, iodine material density image. *D*, Perfusion color map was also created from dual-energy CT data set and shows perfused bowel in gold, a color that is absent from ischemic segment *(Fig 4 continues).*

Figure 4 (continued)

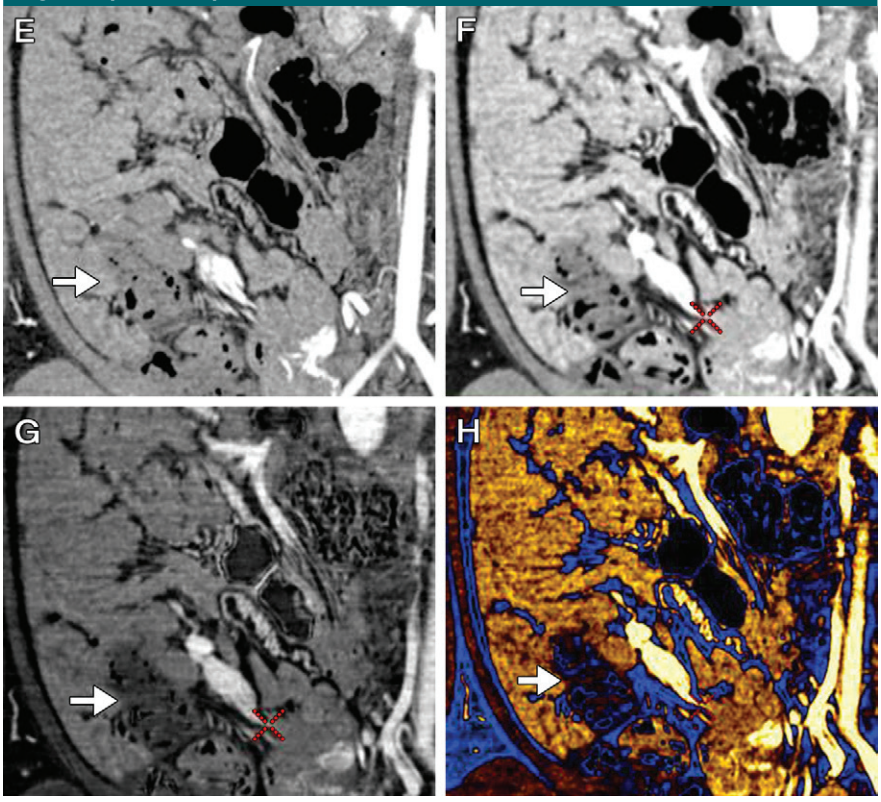

Figure 4 *(continued)*: Coronal reformatted images of the same segment are shown on, *E*, conventional 120-kVp, *F*, virtual monoenergetic 51-keV, *G*, iodine material density, and, *H*, perfusion color map reconstructions. In this case, dual-energy imaging was performed after conventional imaging, which accounts for difference in contrast agent distribution. Half of the animals were imaged in this order, and the other half were imaged with dual-energy CT in the earlier phase and conventional imaging in the later phase to account for potential contribution of slight differences in contrast agent timing bowel wall attenuation.

supported the anecdotal observations of these authors.

Authors of prior investigations (23–25) demonstrated the utility of dual-energy CT for the detection of other hypoenhancing abnormalities such as pancreatic adenocarcinoma and hypovascular liver lesions. These studies have shown that the conspicuity of hypoenhancing lesions is increased relative to adjacent normally enhancing tissue when dual-energy CT is used. The increased conspicuity is due to the higher attenuation of the adjacent normally enhancing liver and pancreas at lower viewing energies and the resultant larger attenuation differences. Despite the increasing use and accessibility of dual-energy CT technology, investigations of potential applications for bowel ischemia remain limited to date.

Dual-energy CT also could add value in the diagnosis of hemorrhagic bowel infarction. In hemorrhagic infarction, which is seen more often with venous occlusion, the bowel wall attenuation may be high on unenhanced CT images due to the presence of blood (26,27). On a conventional contrast-enhanced image, if no unenhanced sequences were performed, it is difficult to determine whether high attenuation in the bowel wall is due to blood or normal contrast enhancement. Dual-energy CT not only has the capability of creating a virtual unenhanced series but also can allow separation of iodine from other materials, such as blood (28). A dual-energy CT scan could allow differentiation between hemorrhage and iodine in the bowel wall. The possibility of creating a virtual unenhanced series would not only be helpful for troubleshooting, as in the case of hemorrhagic infarction, but also could obviate a precontrast series in patients suspected of having mesenteric ischemia when the burden of arterial atherosclerotic disease also must be evaluated.

Limitations of our study included the relatively small number of animals imaged, although in comparison tests, the data were sufficient to allow detection of the most notable differences (51 keV vs 120 kVp). The study may have been underpowered for detection of differences between other groups (65 or 70 keV vs 120 kVp), but if additional samples would have revealed statistical differences between these other groups, it is unlikely that those differences would have been significant based on their relatively small magnitude (< 10 HU). Our examinations were performed exclusively with a single-source fast-switching dual-energy scanner, although we believe similar results would be achievable with a dual-source scanner. We did not give animals positive oral contrast agents, which are used in many centers for abdominal imaging. Although positive oral contrast agents might limit the potential benefit of scanning with dual-energy CT for bowel evaluation, a negative oral contrast agent could allow further improvement in detection of the ischemic bowel with dual-energy CT.

In clinical practice, the performance of dual-energy CT for the detection of bowel ischemia may be influenced by several factors including scanner and software availability and radiologist familiarity with the technique. When bowel ischemia is clinically suspected, images must be obtained and interpreted emergently, and dual-energy CT processing and viewing time may slightly increase turnaround time for results.

In summary, the use of dual-energy CT may help improve early detection of bowel ischemia by increasing conspicuity of underperfused tissues on

Figure 5

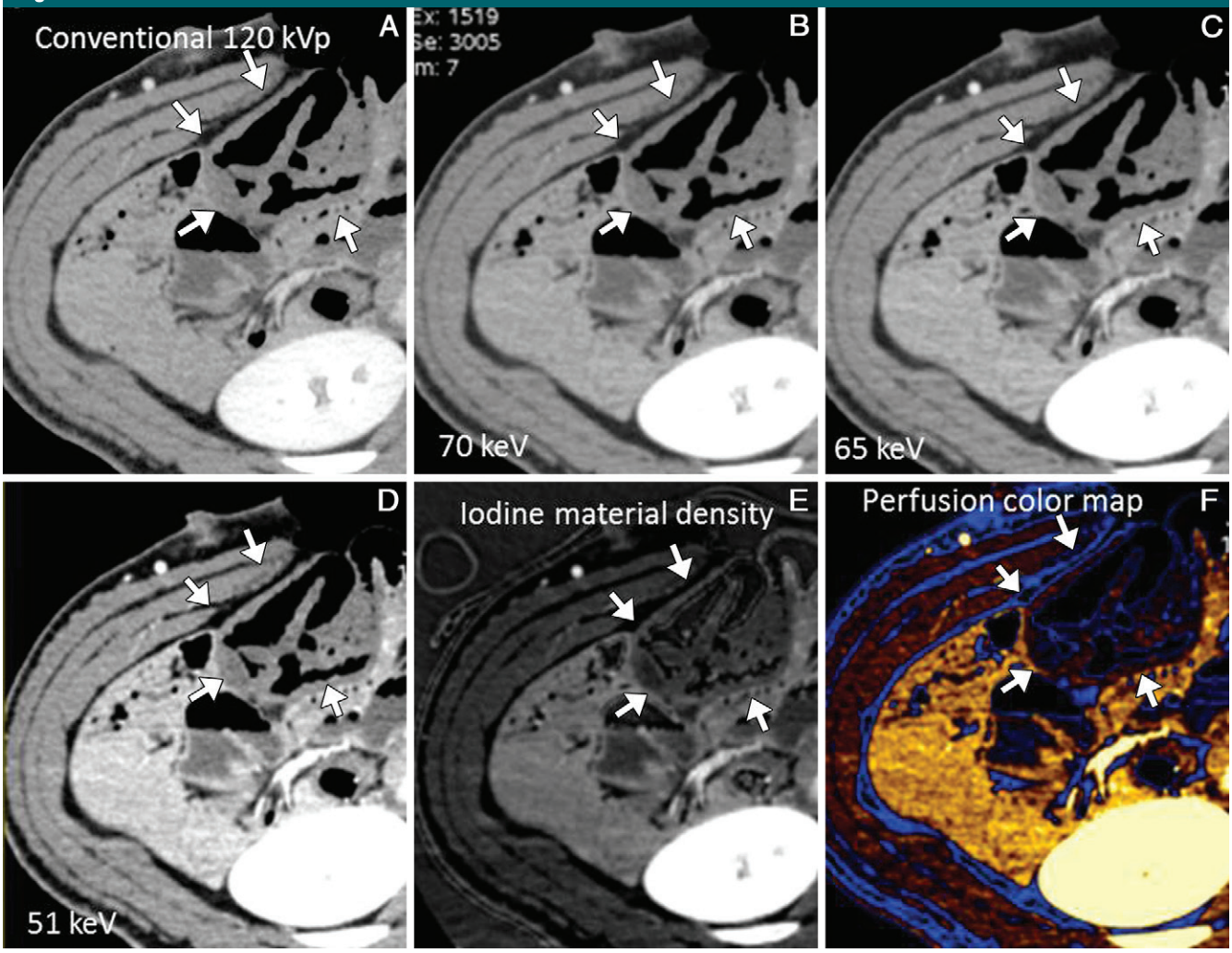

Figure 5: Axial contrast-enhanced CT images show an ischemic segment of swine bowel in the right upper quadrant (arrows). This hypoperfused segment is less conspicuous on, *A*, conventional 120-kVp, *B*, 70-keV, and *C*, 65-keV images than on, *D*, 51-keV, and, *E*, iodine material density images. *F*, Perfusion color map shows absence of gold color in wall of ischemic segment, which is indicative of underperfusion. This image was obtained in early delayed phase, and although these data were not used for our analysis, conspicuity differences are well demonstrated.

Mean Attenuation and Iodine Concentration, Attenuation Difference, Noise, and CNR of Ischemic and Perfused Bowel Segments

	Iodine Concentration (mg/cm^3)			Attenuation (HU)				
Image Type	Ischemic	Perfused	Difference	Ischemic	Perfused	Difference	Image Noise (HU)	CNR
Iodine material density	6.4 ± 2.4	23.5 ± 6.4	17.1	. . .	. . .	. . .	3.1 ± 0.7	4.9 ± 1.6
51 keV	. . .	. . .	. . .	57.4 ± 8.6	149.1 ± 27.4	91.7	20.4 ± 3.8	4.3 ± 1.8
65 keV	. . .	. . .	. . .	39.4 ± 10.5	94.4 ± 12.5	55.0	12.2 ± 2.3	4.4 ± 1.8
70 keV	. . .	. . .	. . .	38.1 ± 10.1	83.9 ± 11.3	45.8	11.1 ± 1.6	4.1 ± 1.7
120 kVp conventional	. . .	. . .	. . .	38.2 ± 13.1	85.8 ± 10.8	47.6	22.7 ± 4.2	2.1 ± 0.6

Note.—Unless otherwise indicated, data are means ± standard deviation.

low–kiloelectron volt and iodine material density images. Additional investigation of dual-energy CT is warranted in humans, ideally in a prospective fashion, to evaluate its potential to improve the sensitivity and specificity of CT for detection of early small-bowel ischemia.

Disclosures of Conflicts of Interest: T.A.P. disclosed no relevant relationships. **C.L.B.** Activities related to the present article: disclosed no relevant relationships. Activities not related to the present article: consultancy and stock/stock options with NeuWave Medical and SympleSurgical, patents pending with Wisconsin Alumni Research Foundation and NeuWave Medical. Other relationships: disclosed no relevant relationships. **M.G.L.** Activities related to the present article: disclosed no relevant relationships. Activities not related to the present article: grant for radiology research fellowship from GE Medical. Other relationships: disclosed no relevant relationships. **L.A.S.** disclosed no relevant relationships. **B.J.W.** disclosed no relevant relationships. **F.T.L.** Activities related to the present article: disclosed no relevant relationships. Activities not related to the present article: board membership and patents with NeuWave Medical, patents and royalties from Covidien. Other relationships: disclosed no relevant relationships.

References

1. Brandt LJ, Boley SJ. AGA technical review on intestinal ischemia. American Gastrointestinal Association. Gastroenterology 2000; 118(5):954–968.
2. Kougias P, Lau D, El Sayed HF, Zhou W, Huynh TT, Lin PH. Determinants of mortality and treatment outcome following surgical interventions for acute mesenteric ischemia. J Vasc Surg 2007;46(3):467–474.
3. Taourel PG, Deneuville M, Pradel JA, Régent D, Bruel JM. Acute mesenteric ischemia: diagnosis with contrast-enhanced CT. Radiology 1996;199(3):632–636.
4. Zalcman M, Sy M, Donckier V, Closset J, Gansbeke DV. Helical CT signs in the diagnosis of intestinal ischemia in small-bowel obstruction. AJR Am J Roentgenol 2000;175(6):1601–1607.
5. Kirkpatrick ID, Kroeker MA, Greenberg HM. Biphasic CT with mesenteric CT angiography in the evaluation of acute mesenteric ischemia: initial experience. Radiology 2003;229(1):91–98.
6. Sheedy SP, Earnest F 4th, Fletcher JG, Fidler JL, Hoskin TL. CT of small-bowel ischemia associated with obstruction in emergency department patients: diagnostic performance evaluation. Radiology 2006;241(3):729–736.
7. Barmase M, Kang M, Wig J, Kochhar R, Gupta R, Khandelwal N. Role of multidetector CT angiography in the evaluation of suspected mesenteric ischemia. Eur J Radiol 2011;80(3):e582–e587.
8. Geffroy Y, Boulay-Coletta I, Jullès MC, Nakache S, Taourel P, Zins M. Increased unenhanced bowel-wall attenuation at multidetector CT is highly specific of ischemia complicating small-bowel obstruction. Radiology 2014;270(1):159–167.
9. Kruger RA, Riederer SJ, Mistretta CA. Relative properties of tomography, K-edge imaging, and K-edge tomography. Med Phys 1977;4(3):244–249.
10. Riederer SJ, Mistretta CA. Selective iodine imaging using K-edge energies in computerized x-ray tomography. Med Phys 1977;4(6):474–481.
11. Nakayama Y, Awai K, Funama Y, et al. Abdominal CT with low tube voltage: preliminary observations about radiation dose, contrast enhancement, image quality, and noise. Radiology 2005;237(3):945–951.
12. Kalva SP, Sahani DV, Hahn PF, Saini S. Using the K-edge to improve contrast conspicuity and to lower radiation dose with a 16-MDCT: a phantom and human study. J Comput Assist Tomogr 2006;30(3):391–397.
13. Institute of Laboratory Animal Resources, Commission of Life Sciences, National Research Council. Guide for the care and use of laboratory animals. Washington, DC: National Academy Press, 1996.
14. Potretzke TA, Brace CL, Lubner MG, Sampson L, Willey B, Lee FT Jr. Dual energy CT improves visibility of early small bowel ischemia compared to conventional CT in a swine model [abstr]. Abdom Imaging 2013; 38(4):624.
15. Pinheiro JC, Bates DM. Mixed-effects models in S and S-PLUS. New York, NY: Springer, 2000:133–199.
16. Pinheiro JC, Bates DM. DebRoy S, Sarkar D. Linear and nonmaterial mixed effects models, R package version 3.1-110. http://cran.r-project.org/web/packages/nlme/index.html. Published 2012. Accessed April 1, 2014.
17. R Core Team. R: A language and environment for statistical computing. R Foundation for Statistical Computing, Vienna, Austria. http://www.R-project.org/. Published 2013. Accessed April 1, 2014.
18. Fletcher JG. CT enterography technique: theme and variations. Abdom Imaging 2009;34(3):283–288.
19. Fletcher JG, Takahashi N, Hartman R, et al. Dual-energy and dual-source CT: is there a role in the abdomen and pelvis? Radiol Clin North Am 2009;47(1):41–57.
20. Graser A, Johnson TRC, Chandarana H, Macari M. Dual energy CT: preliminary observations and potential clinical applications in the abdomen. Eur Radiol 2009;19(1):13–23.
21. Yeh BM, Shepherd JA, Wang ZJ, Teh HS, Hartman RP, Prevrhal S. Dual-energy and low-kVp CT in the abdomen. AJR Am J Roentgenol 2009;193(1):47–54.
22. De Cecco CN, Darnell A, Rengo M, et al. Dual-energy CT: oncologic applications. AJR Am J Roentgenol 2012;199(5 Suppl):S98–S105.
23. Macari M, Spieler B, Kim D, et al. Dual-source dual-energy MDCT of pancreatic adenocarcinoma: initial observations with data generated at 80 kVp and at simulated weighted-average 120 kVp. AJR Am J Roentgenol 2010;194(1):W27–W32.
24. Robinson E, Babb J, Chandarana H, Macari M. Dual source dual energy MDCT: comparison of 80 kVp and weighted average 120 kVp data for conspicuity of hypo-vascular liver metastases. Invest Radiol 2010;45(7):413–418.
25. Patel BN, Thomas JV, Lockhart ME, Berland LL, Morgan DE. Single-source dual-energy spectral multidetector CT of pancreatic adenocarcinoma: optimization of energy level viewing significantly increases lesion contrast. Clin Radiol 2013;68(2):148–154.
26. Wiesner W, Khurana B, Ji H, Ros PR. CT of acute bowel ischemia. Radiology 2003; 226(3):635–650.
27. Whitehead R. The pathology of ischemia of the intestines. Pathol Annu 1976;11:1–52.
28. Johnson TRC, Krauss B, Sedlmair M, et al. Material differentiation by dual energy CT: initial experience. Eur Radiol 2007; 17(6):1510–1517.